JTTEE5 19:765–778
DOI: 10.1007/s11666-009-9385-3
1059-9630/$19.00 © ASM International

Better Quality Control: Stochastic Approaches to Optimize Properties and Performance of Plasma-Sprayed Coatings

Robert B. Heimann

(Submitted June 18, 2009; in revised form July 25, 2009)

Statistical design of experiment (SDE) methodology applied to design and performance testing of plasma-sprayed coatings follows an evolutionary path, usually starting with classic multiparameter screening designs (Plackett-Burman), and progressing through factorial (Taguchi) to limited response surface designs (Box-Behnken). Modern designs of higher dimensionality, such as central composite and D-optimal designs, will provide results with higher predictive power. Complex theoretical models relying on evolutionary algorithms, and application of artificial neuronal networks (ANNs) and fuzzy logic control (FLC) allow estimating the behavior of the complex plasma spray environment through validation either by key experiments or first-principle calculations. In this review, paper general principles of SDE will be discussed and examples be given that underscore the different powers of prediction of individual statistical designs. Basic rules of ANN and FLC will be briefly touched on, and their potential for increased reliability of coating performance through stringent quality control measures assessed. Salient features will be reviewed of studies performed to optimize thermal coating properties and processes reported in the pertinent literature between 2000 and the present.

Keywords Artificial Neuronal Networks, D-optimal designs, fuzzy logic control, statistical design of experiments, Taguchi designs

1. Quality Implementation

Owing to the chaotic nature of the plasma spray process, the structure and properties of coatings produced by this technique are subject to stochastic fluctuations. Consequently, many intrinsic and extrinsic parameters and their generally complex interactions affect in a nondeterministic way the properties and hence the in-service performance of plasma-sprayed coatings. It has been good practice for a long time to select those sets of parameter that are known to influence coating structure and properties to the largest extent, and to run a series of experiments with these statistically distributed parameters. As a result, the directions and magnitude of trends can be estimated with confidence, and a protocol established to manufacture coatings on an industrial scale that will adhere to stringent quality control measures and be monitored by statistical process control (SPC).

Robert B. Heimann, Professor Emeritus of Applied Mineralogy and Materials Science, Am Stadtpark 2A, 02826 Görlitz, Germany. Contact e-mail: robert.heimann@ocean-gate.de.

An important aspect of industrial plasma spray technology is the development and implementation of quality control and assurance protocols to ensure consistency of properties. Because a multitude of spray parameters can potentially influence coating properties in a nonlinear way, parameter optimization involves statistical experimental design procedures. Such procedures provide a maximum of information on the anatomy and behavior of a system with a minimum number of experiments. This very favorable experimental economy will save time and resources, and hence money. General principles of multifactorial analyses and several case studies have been reviewed by Bisgaard (Ref 1), Heimann (Ref 2), and Pierlot et al. (Ref. 3).

Total Quality Management (TQM) is a complex system of several innovative and interacting disciplines including enlightened management philosophy (''Achieving success through the work of others''), psychology of work organization (''Control the process, not the people''), and engineering and scientific expertise. It involves the concept of continuous improvement (CI) (in Japanese: Keizen; see for example, Ref 4) that can be divided into three groups: implementing *quality tools*, developing *quality philosophy*, and executing *management style*. To be successful in TQM, it is mandatory that all three units are closely linked, and interact smoothly and continuously since it is generally not sufficient to improve only one or two of these pillars of TQM. Thus TQM is more than just a quality evolution but a system of CI of the process (CPI) and the product.

Statistical design of experiments (SDEs) is the backbone quality tool of TQM. Using SDE, many of the factors can be screened out that crucially control the process and/or the product performance. Closely associated with SDE is statistical experimental strategy (SES) that attempts to answer important questions at the start of a research program such as the number of experiments needed, the number and ranges of the parameters to be selected, the costs of the program, the equipment and manpower needed, the duration, etc. Likewise important is the initial selection of the quality characteristics that the experimental program is supposed to satisfy, i.e., the customer expectation. This will allow declaring with confidence what exactly the analyses of the experimental data will teach the experimenter about the system under investigation. Linking SDE with SES will establish a successful way to plan and execute experiments at conditions that will result in meaningful, i.e., valid and statistically accurate and precise conclusions.

An important element of TQM is *quality function deployment* (QFD). The customer defines the ''quality'' of the coating in usually nonengineering terms, i.e., a set of desired properties that must be unequivocally adhered to. This information supplied by the customer is analyzed by the R&D team and transformed into engineering design and specification requirements. If this is being done properly, the final coating will have the predefined ''quality'' even if the customer as a nonexpert cannot explain clearly this desired ''quality'' in realistic engineering terms.

2. Principles and Examples of Statistical Design of Experiments

2.1 Screening Designs

In a real experimental program, the screening designs, in particular Plackett-Burman-type designs (Ref 5), are the starting point for any investigation of a completely unknown system. They serve to screen out the few really important, i.e., statistically significant variables that stand out over a background of a large number of possible ones with a minimum of test runs hence separating true signals from experimental noise. Plackett-Burman designs are fractions of an $N = 2^p$ factorial for which N is a multiple of 4. Although they allow a tremendous reduction in experimentation, there is no estimate of synergistic nonlinear parameter interactions. In fact, only estimates of main effects clear of each other can be obtained. Examples of calculation of factor effects and determination of factor significance can be found in Ref 2.

Generally at the outset of an experimental investigation, there already exists basic knowledge about the influence of parameters commonly varied within a design matrix. Hence there is a tendency to skip screening experiments and immediately proceed to designs with higher power of resolution such as those discussed below. However, there may be costly pitfalls as this will potentially lead to type II (ß) errors, i.e., the conclusion that a factor effect is not significant when it actually is. A recent example of successful application of an 8-run Plackett-Burman screening design is the optimization of thickness and porosity of glazes with confidential composition flame sprayed (oxyacetylene, stoichiometric ratio 0.6, total gas flow rate 50 slpm) onto hydraulic binder substrates (Ref 6). The four factors investigated include (i) powder feed rate (20 or 30 g/min), (ii) stand-off distance (90 or 150 mm), (iii) traverse speed (7 or 15 cm/s), and (iv) scanning offset (1 or 3 mm/pass). Coatings thickness varied between 374 ± 34 and 1191 ± 34 μm and coating porosity between 9 and 20 vol.%. It was found that the most significant factor was the stand-off distance: low stand-off produced maximum coating thickness with minimum porosity.

2.2 Factorial Designs

2.2.1 Full Factorial Designs. Factorial designs permit the estimation of the main (linear) effects of several factors, X_i simultaneously and clear of two-factor interactions, $\{X_iX_j\}$. The total number of experiments, N is obtained by running experiments at all combinations of the p factors with L levels per factor, i.e., $N = L^p$ for a full factorial design. In particular, two-level factorial designs ($L = 2$) are highly useful for a wide variety of problems. They are easy to plan and to analyze, and readily adaptable to both continuous and discrete factors. Such designs provide adequate prediction models for responses without a strong nonlinear behavior in the experimental region. However, for best results the responses Y should be continuous, and have uniform and independent errors. This means that (i) the experimental error must have approximately the same magnitude at all experimental points, and that (ii) the size and sign of error at any one experimental point must not be affected by the sizes and signs of errors that occur at other experimental points. If requirement (i) cannot be guaranteed a logarithmic transformation of the responses Y is often advisable. With factor coding as discussed above, using the so-called Yates order (Ref 7) and randomization of the experimental trials, factor effects for each main effect and two-factor interaction are calculated. The computation of factor effects and residuals can also be quickly and accurately accomplished using the IYA (inverse Yates algorithm; Ref 8).

Recent work using full factorial designs includes the deposition of NiAl 95-5 and NiAl 65-35 coatings with and without aluminum or zinc bond coats on graphite reinforced polymer surfaces deposited by plasma, flame, and wire arc spraying to optimize microhardness, erosion resistance, and electrical conductivity. The effects of coating materials composition, power level, and standoff distance were studied using full factorial 2^3 designs (Ref 9). An identical design was applied to mimic the microstructure of HVOF-sprayed MCrAlY bond coats on IN738 substrates by using APS technology to improve oxidation and spallation life. The parameters varied were the secondary gas flow rate, the arc current, and the powder feed rate. Desirable levels of porosity and

oxidation approaching those typical for HVOF coatings were achieved by reducing the particle size in a second optimization design experiment (Ref 10).

2.2.2 Fractional Factorial Designs. If the number of parameters p to be estimated becomes larger than five or six, a full factorial may not be appropriate anymore for reasons of experimental economy. Then, fractions of a full factorial can be run, i.e., $N = 2^{p-q}$. In particular, half-fraction of full factorials, $N = 2^{p-1}$ estimate main effects and two-factor interactions clear of each other.

Fractional factorial designs are useful in the following situation (Ref 11):

- when some interactions can be reasonably assumed nonexistent from prior knowledge,
- in screening operations where it is expected that the effects of all but a few of the factors will be negligible,
- where blocks of experiments are run in sequence, and ambiguities remaining at an earlier stage of experimentation can be resolved by later blocks of experiments, and
- when some factors that may interact are to be studied simultaneously with others whose influence can be described through main effects only.

Figure 1 shows response surfaces depicting the dependence of the thickness of APS Cr_2O_3 coatings on the plasma spray parameters arithmetic surface roughness of the substrate X_1 (4; 20 μm), plasma power X_2 (29; 39 kW), powder feed rate X_3 (10; 40%), powder grain size X_4 (−45 + 25; −75 + 25 μm) and spray distance X_5 (80; 120 mm) varied according to a 2^{5-1} fractional factorial design of resolution V (Ref 12).

It could be shown that the coating thickness depends in a statistically significant way on the main effects X_1 to X_4 and on the two-factor interactions X_1X_4, X_1X_5, and X_3X_4 yielding the regression polynomial

$$Y_{\text{thickness}} = 23 - 15X_1 + 18X_2 + 70X_3 - 27X_4 - 15X_1X_4 + 34X_1X_5 - 20X_3X_4. \quad \text{(Eq 1)}$$

Interpretation of the contour plots shown in Fig. 1 provides deep insight into the interaction of the various plasma spray parameters and hence the anatomy of the system. The X_1X_5 plot (Fig. 1a) yields a saddle (col) surface for intermediate parameter setting ($X_2 = 34$ kW, $X_3 = 25\%$, and $X_4 = 60$ μm) resulting in average coating thicknesses between 60 and 65 μm (yellow field). Only with increasing substrate roughness and spray distance the

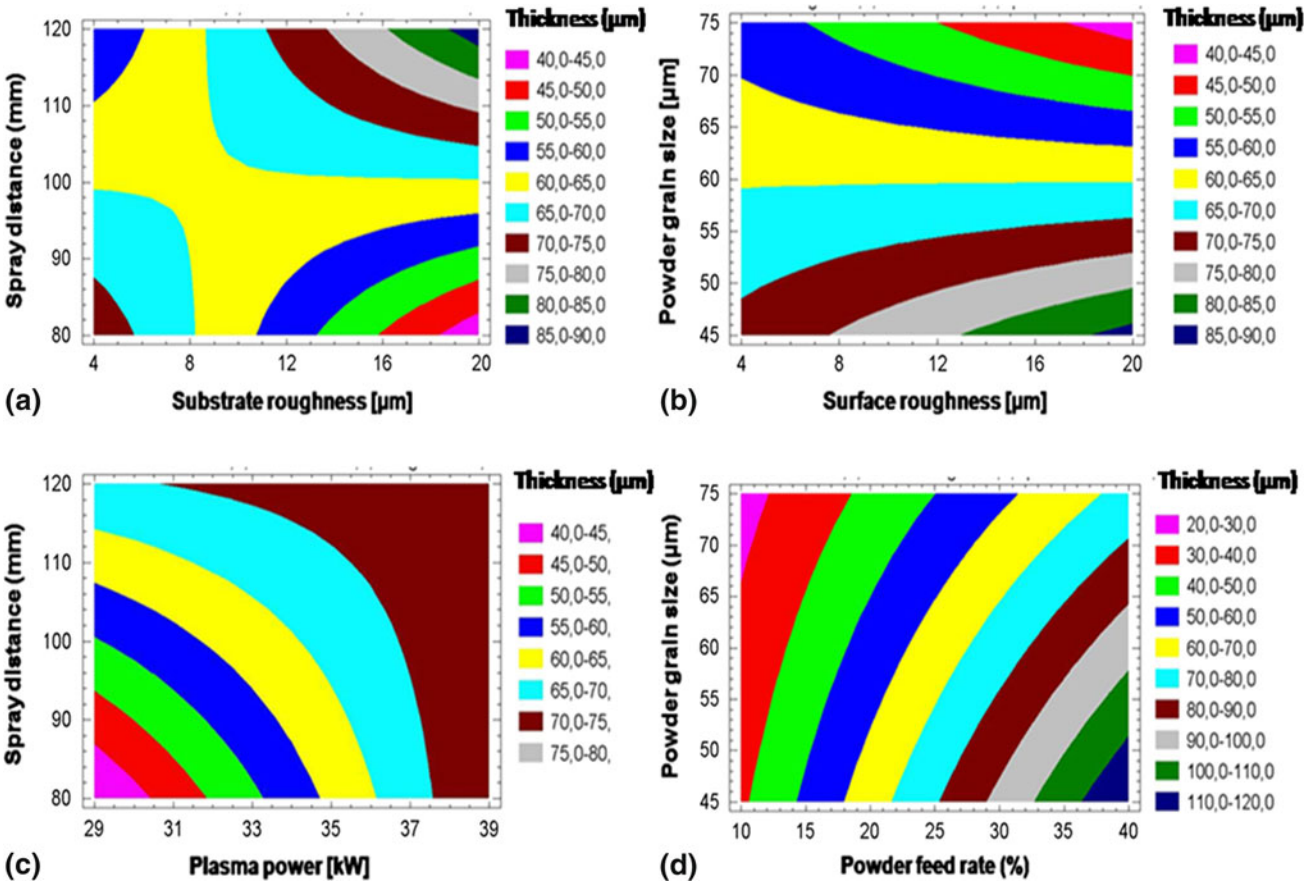

Fig. 1 Response surface contours showing the dependence of the thickness of APS Cr_2O_3 coatings deposited on steel St37 on the arithmetic surface roughness of the substrate (X_1), plasma power (X_2), powder feed rate (X_3), powder grain size (X_4), and spray distance (X_5) (*Courtesy*: Dipl.-Min. Martin Erne, Leibniz-Universität Hannover, Germany)

thicknesses are varying appreciably caused by reduced heat dissipation of the rougher surfaces at short spraying distance. The X_1X_4 plot (Fig. 1b) obtained for constant parameters X_2 (34 kW), X_3 (25%), and X_5 (100 mm) shows that the coating thickness strongly increases with decreasing two-factor interaction X_1X_4. The reason for the pronounced effect of the substrate roughness X_1 relates to the reduced adhesion of the coarse powder particles at the very rough surface as well as a possible effect of surface activation and insufficient heat dissipation. On the other hand, during spraying of fine powder particles, the surface activation provides excellent adhesion of the particles and thus large coating thickness. Although the two-factor interaction X_2X_5 was found to be nonsignificant during evaluation of the factor effects, its response surface (Fig. 1c) obtained for intermediate parameter setting ($X_1 = 12$ μm, $X_3 = 25\%$, and $X_4 = 60$ μm) shows that the coating thickness yields a high gradient at low plasma power values. The low coating thickness at low spray distance is likely related to insufficient melting of the powder particles at low enthalpies and the fact that a high proportion of nonmelted particles will erode the already deposited material. Higher plasma powers result in a higher proportion of melted particles and consequently in higher coating thickness even at low spray distance. Finally, the X_3X_4 plot ($X_1 = 12$ μm, $X_2 = 34$ kW, and $X_5 = 100$ mm) reveals that the coating thickness increases steeply with decreasing two-factor interaction X_3X_4. The maximum coating thickness will be realized for fine, well-melted particles that are deposited with high feed rates on a surface with low roughness (Fig. 1d).

A fractional factorial design at two levels with seven input parameters (powder size, fuel gas flow rate, fuel-to-oxygen ratio, spray distance, carrier gas flow rate, air flow rate, and traverse speed) was applied to optimize five coating properties: hardness, microstructure, adhesion strength, tensile strength, and coating deposition rate of HOVF-sprayed WC-Co and WC-CoCr coatings as a replacement for hard chrome plating on aircraft landing gear (Ref 13). During evaluation of the coating properties, a pre-DOE parameter set was established; the test matrix was later modified by experimental results to determine the range of test conditions needed to provide reasonable, measurable ranges of wear rates for the material combinations in tests typically averaging not more than 48 h. Then an L_{12} Taguchi matrix was employed with nine parameters to evaluate the major potential sliding and fretting wear factors, and finally an $L_8(2^{4-1})$ Taguchi matrix to quantify the relative contributions to sliding wear performance of the major wear factors identified in the L_{12} matrix. It was estimated that the use of HVOF for C-130 landing gear components will result in a net decrease in annual operating costs. The primary difference between the deposition equipment used is the fuel type utilized. The Diamond Jet 2600 uses hydrogen as a fuel, the Diamond Jet 2700 uses propylene, and TAFA JP5000 uses kerosene. The difference in fuel costs is the reason that the Tafa equipment shows a more positive NPV. A reduced labor requirement with HVOF implementation was the primary cost driver in this analysis.

2.2.3 Taguchi Designs. These designs are basically full or fractional factorial designs using robust orthogonal arrays of factors (Ref 14). The structure of the experimental matrix frequently consists of an inner and an outer array. The former contains the control factors, the latter the disturbance variables, i.e., external factors subject to unavoidable and uncontrollable oscillations around the set point that will likely influence the process results. The measure of the variation around the set point is the signal-to-noise ratio $S/N = \log(\overline{Y}^2/S^2)$, where S effect of signal, N effect of noise, $\overline{Y}$ average of the response, and S standard deviation.

The aim of the design is to determine those combinations of control factors that minimize the influence of the disturbance variables while maintaining the desired set point. While Taguchi designs are very popular in the industrial praxis owing to their simplicity and easily comprehensible internal structure, they have drawn criticism from statisticians related to the overly simplistic definition of the signal-to-noise ratio, deficiencies in statistical efficiency of the composite experimental design matrix, and also the risk of confounding main effects and factor interactions (Ref 15).

Saravanan et al. (Ref 16) used an $L_{16}(2^4)$ full factorial Taguchi design to optimize the microstructure (porosity, surface roughness, and microhardness) of plasma-sprayed alumina coatings by varying four parameters (argon gas flow rate, powder feed rate, plasma arc current, spray distance) at two levels. Low porosity was obtained for high argon gas flow rate and arc current, high hardness resulted for high argon gas flow rate and low spray distance, and low surface roughness was found for high argon gas flow rate, arc current and spray distance, and low powder feed rate. The same authors applied an $L_8(2^{4-1})$ fractional factorial Taguchi design to evaluate the effects of four detonation spray process parameters (acetylene-to-oxygen ratio, powder carrier gas flow rate, detonation frequency, and stand-off distance) on surface roughness, porosity, microhardness, and abrasion mass loss of alumina coatings. High fuel-to-oxygen ratio and low stand-off distance promote coatings with higher hardness, lower porosity, and lower abrasion mass loss (Ref 17-19).

Kucuk et al. (Ref 20) examined the mechanical properties of Y-stabilized zirconia thermal barrier coatings (TBCs), plasma-sprayed onto a NiCrAlY bond coat using a 9-run $L_8(2^{4-1})$ fractional Taguchi design with one center point as well as a 17-run $L_{16}(2^4)$ full Taguchi design with one center point, varying the YSZ top coat thickness, t_{TC} (300 or 500 μm), NiCrAlY bond coat thickness, bond coat thickness, t_{BC} (100 or 250 μm), substrate temperature, T_S (273 or 393 K) and stand-off distance, X (80 or 100 mm). A multilinear regression analysis on the four-point bending yield stress σ_{YC} and elastic modulus E_C suggested that coatings with thinner bond and top coats sprayed onto a cold substrate lead to coatings with maximum bending yield stress and modulus. The calculated polynomials are

$$\sigma_{YC}(\text{MPa}) = 461 - 0.71t_{BC} - 0.47T_S \text{ (s.d.} = \pm 106 \text{ MPa)}, \quad \text{(Eq 2)}$$

$$E_C(\text{GPa}) = 198 - 0.31t_{BC} - 0.15T_S - 0.07t_{TC} \quad (\text{s.d.} = \pm 40\ \text{GPa}). \qquad \text{(Eq 3)}$$

Highly durable TBCs of low thermal conductivity were deposited by a solution precursor plasma spray (SPPS) process (Ref 21). In this study, an $L_{27}(3^3)$ Taguchi full factorial design was employed to optimize the process. The spallation lifetime of SPPS TBCs (ZrO_2-7wt.% Y_2O_3; 250 μm) on a CoCrAlY (100 μm) bond-coated Ni-based superalloy substrate deposited under optimized processing conditions was reported to be more than 2.5 times that of a conventional plasma-sprayed TBC using the same substrate and bond coat. The superior durability of SPPS TBCs was thought to be associated with their microstructures that include (i) a ceramic matrix containing micrometer- and nanometer-sized pores, (ii) the presence of very fine splats (0.5-5 mm), (iii) through-thickness cracks, and (iv) improved ceramic-to-bond coat adhesion. The in-service failure of coating by buckling spallation occurs within the ceramic top coat, near the ceramic-bond coat interface.

Application of Taguchi design methodology to deposit bioconductive hydroxyapatite (Ref 22) and titania (Ref 23) coatings on Ti6Al4V alloy substrates by plasma spraying showed that primary gas flow rate and spray distance were the decisive factors that influence coating surface roughness and porosity that are both known to control osteoblast vitality, adhesion, and proliferation.

CrC-NiCr and FeNiCr alloy coatings intended for protection of aluminum injection mould tooling were deposited by HVOF and APS, and their adhesion optimized using an L_{18} five parameter, three-level fractional Taguchi design. The five parameters investigated were the flow rates of oxygen, propane and air as well as the powder feed rate, and the stand-off distance (Ref 24). The coating bond strengths were prominently dependent on powder feed rate and propane gas flow rate.

A thorough study was recently performed (Ref 25) of the influence of seven independent parameters including solid content (10% or 30%), auxiliary gas type (He or H_2), complex torch condition, injection feed rate (1.3 or 1.8 kg/h), powder grain size (nano- or microsized), substrate roughness (achieved by blasting with #24 or #60 mesh alumina grit), and traverse speed (0.6 or 2 m/s) on six dependent response properties including particle temperature and velocity, coating porosity, horizontal and vertical crack spacing, and deposition rate of alumina-zirconia coating deposited by axial injection suspension plasma spraying (SPS). Presumably a Taguchi-type fractional factorial design was applied even though the contribution did not reveal the number of runs from which the degree of fractionation could have been determined. The most influential variables were those that directly affect particle velocity and temperature, i.e., type of auxiliary gas and torch conditions. More specifically, particle velocity was predominately controlled by intrinsic parameters such as total gas flow rate, plasma power, and plasma gas composition whereas particle temperature was mainly dependent on extrinsic feed stock-related parameters such as solid content, particle size, and powder feed rate. This is well in accord with the hierarchical parameter dependence shown in Fig. 2 (Ref 26) considering that plasma temperature appears to control particle velocity.

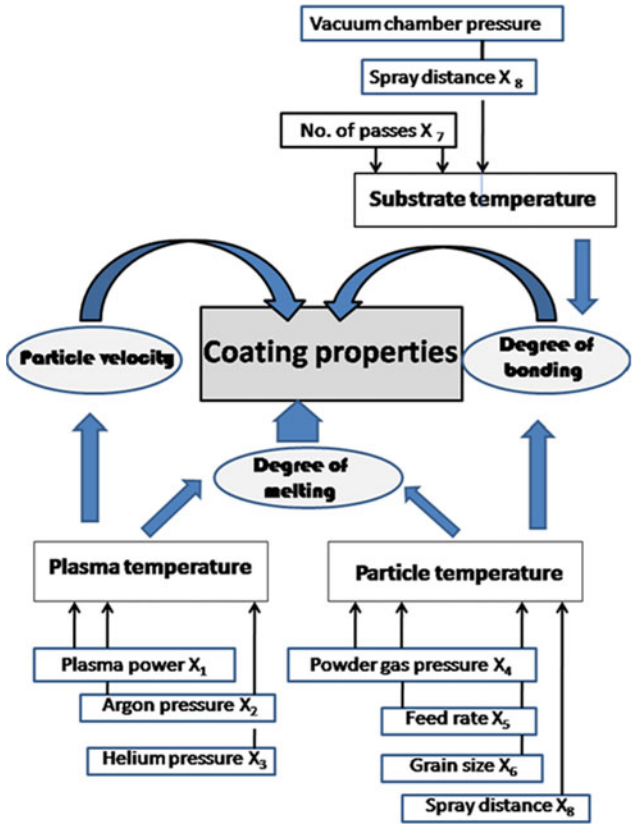

Fig. 2 The development of coating properties shows a three-tiered hierarchy relating extrinsic parameters X_i and intrinsic plasma, particle, and coating properties. *First level*: intrinsic plasma spray parameters X_1 to X_8, *second level*: temperatures of plasma, particles and substrate, *third level*: particle velocity, degree of melting, and degree of bonding (Ref 26)

To optimize the bond strength of a self-fluxing NiCrBSi coatings deposited by flame spraying onto mild steel, a Taguchi fractional factorial design with four variables (preheating temperature of substrate, spraying distance, type of oxy-acetylene flame, and surface roughness of the substrate) was applied and validated by additional confirmatory experiments performed with the optimum parameter settings (Ref 27).

A Taguchi $L_{16}(2^{7-3})$ design in parameters plasma current, argon flow rate, hydrogen flow rate, spraying distance, spraying angle, cooling, and traverse speed was utilized to optimize the deposition efficiency, roughness, porosity, and thermal conductivity of TBCs produced from plasma-sprayed hollow Y-PSZ spheres. Special attention was devoted to the relationship between the thermophysical properties of TBCs and their porous network, described by image analysis. Since even for coatings produced with the same type of powder the thermal conductivity cannot be linked with a single parameter characterizing their porosity, details of the porous network, i.e., the relative amount and orientation of macropores

and microcracks have to be considered. In coatings dominated by macropores, the thermal conductivity decreases with increasing volumetric amount of macropores whereas in coatings dominated by microcracks the thermal conductivity is related to the proportion of microcracks oriented parallel to the substrate-coating interface (Ref 28).

2.3 Box-Behnken Designs

Box-Behnken designs (Ref 29) are incomplete three-level factorial designs that allow an estimation of the coefficients in a second-degree graduating polynomial. They employ subsets of the corresponding full three-level factorial, 3^p. For example, the three-factor design uses only 13 of the 27 points of the full factorial 3^3 with two extra replicates of the center points added, for a total of 15 experimental points of a spherical space-filling* and rotatable design. Another desirable feature of such designs with $p > 4$ is the possibility to run it in separate blocks of experiments. Such *orthogonal blocking* permits to subtract out the effect of a shift of response between blocks, and thus to remove bias errors due to differences in extraneous variables not considered in the design. The 15 data points in the three-factor Box-Behnken design are five more than the minimum number of 10 required to estimate the coefficients of the design (three linear main effects, three parabolic main effects, three-two-factor effects, and one-three-factor effect). Thus, it provides five degrees of freedom for error. Orthogonal blocking is possible for designs from four up to ten factors. Rotatability is associated with the geometrical properties of the design, i.e., the arrangement of the array of data points, except for the center point, to be at the mid-points of the edges or faces of a hypercube whose dimensionality is given by the number of factors considered. Hence all points are situated on a single hypersphere and are thus equidistant from the center. This means that the design is balanced by the mathematical momentum condition. The replicated center point allows (i) to estimate the minimum factor significance, i.e., the inherent experimental error, and (ii) to give constant prediction variances as a function of distance from the center.

It is good experimental strategy to employ such Box-Behnken-type designs at a rather advanced stage of experimentation when the number of potentially significant factors has been narrowed down to three to six continuous factors. As pointed out by Bisgaard (Ref 1), even considering the nonlinearity of responses in plasma-sprayed designs does not warrant, for reasons of experimental economy, three-level factorial designs in the initial stage of experimentation. Thus, second-order effects should be dealt with exclusively when they actually show up in the set of data, and not only because the experimenter suspects that the system under investigation may show some global nonlinearity! When switching from two- to three-level designs any discrete, i.e., noncontinuous factor effect must be considered constant. The response surface obtained through a Box-Behnken RSM-design provides usually a high-quality prediction over a region where linear, parabolic (curvature), and two-factor interactions are needed to describe a response of the system, Y as a function of the coefficients of the independent input parameters X_i obtained by a full quadratic polynomial for p independent parameters:

$$Y = b_0 + \sum b_j X_j + \sum b_{jj,} X_j X_{j'} + \sum b_{jj} X_j^2, \qquad \text{(Eq 4)}$$

with $j > j'$.

Electromagnetic (permittivity) and mechanical (microstructure, hardness, deposition efficiency, fracture toughness, and modulus of rupture) properties of alumina-silica (mullite) coatings were optimized using an RSM approach (Ref 30). A two-step design supported by a nonlinear regression model was applied to optimize the properties of plasma-sprayed stabilized zirconia coatings (Ref 31).

2.4 Designs of Higher Dimensionality

Three levels are the minimum number for each factor to describe accurately nonlinear (curvature) effects. To add additional power of prediction to a Box-Behnken design, it is advisable to use more than three factor levels (see for example Ref 32). One popular class of response surfaces is the *central composite* or Box-Wilson (Ref 33) design that employs five levels for each factor. It is composed of a full two-level factorial 2^3 with added center point(s) plus six star points outside the cube planes defined by the four points of the two-level factorial. The geometrical shape of the resulting five-level design is a tetrakishexahedron whose 14 vortices, i.e., design points surround a k-time replicated center point. This polyhedron is ''cuboidally'' space-filling and can be described as the dual polytope of a cuboctahedral Dirichlet domain (Voronoi polyhedron, Ref 34). Examples of such a design used to determine the fractionality of Cr_2O_3 coatings have been described by Zimmermann (Ref 35), and Reisel and Heimann (Ref 36).

A central composite design was applied by Wang and Coyle (Ref 37) to optimize the process of deposition by solution precursor plasma spraying of porous 8YSZ-40vol.%Ni coatings on sintered PSZ discs intended to be utilized as anodes for SOFCs. A 34-run six-factor fractional small composite design (SCD, Ref 38) of resolution III was used in which the main effects are confounded with two-factor interactions. The six factors investigated were (i) hydrogen gas flow rate (1, 2, or 3 slpm), (ii) arc current (570, 600, or 630 A), (iii) solute flow rate (4, 5.5, or 7 g/min), (iv) solution concentration (0.25, 0.37, or 0.5 mole), (v) distance between nozzle and gun (0.3, 0.8, or 1.3 cm), and (vi) stand-off distance (6, 7, or 8 cm). The coefficients of the quadratic model equations for predicting deposition efficiency (10 significant factors) and porosity (19 significant factors) were fitted and the model adequacy checked by plotting the residuals on a probability net. The models were used successfully to select process parameters which generated coatings with the desired porosity at relatively

*Note that the factorial designs are considered to have a ''cuboidal'' or ''hypercube'' factor space whereas the true response surface designs have a ''spherical'' factor space.

high-deposition efficiency. Physical-based explanations of the empirical relations between the processing parameters and the responses, i.e., the deposition efficiency and the porosity were discussed with reference to experimental observations and theoretical considerations.

Flame-sprayed Al-12wt.%Si coatings on low carbon steel for automotive application were optimized using a central composite design with three factors (oxygen flow rate, acetylene flow rate, and stand-off distance) at three levels. Optimum levels of hardness, thickness, wear rate, and porosity were found for 1.03 m^3/h oxygen flow rate, 0.73 m^3/h acetylene flow rate, and 58 mm stand-off distance (Ref 39).

2.5 Neyer D-Optimal Designs

This test was designed to extract the maximum amount of statistical information from the test samples (Ref 40). Unlike the other statistical test methods described above, this method requires detailed computer calculations to determine the test levels as it uses the results of all the previous tests interactively to compute the next test level.

There are three parts to this test. The first part is designed to ''close-in'' on the region of interest to within a few standard deviations of the mean, as quickly and efficiently as possible. It thus resembles a Plackett-Burman screening test which indeed is D-optimal (Ref 41). The second part of the test is designed to determine efficiently the unique estimates of the parameters. The third part continuously refines the estimates by validation tests once unique optimized estimates have been established. Since the estimate of the standard deviation is used only until overlap of the data occurs, the efficiency of the test is essentially independent of the number of parameters used in the test design.

This experimental design strategy has been applied to optimize thickness and porosity levels of plasma-sprayed tantalum oxide environmental barrier coatings (EBCs) to protect silicon nitride-based ceramics (Ref 42). For the first set of 20 runs, seven parameters based on historical knowledge were varied at two levels: injector angle, plasma power, total gas flow, percent hydrogen in plasma gas, spray distance, carrier gas flow rate, and presence or absence of air cooling, using a D-optimal based software program (Ref 43). During the second round ($N = 16$), three parameters varied in the first set (plasma power, total plasma gas flow, percent hydrogen in the plasma gas) were held constant at their optimized value. To the remaining four parameters, two more were added, powder feeder disk speed and robot scan rate, and varied at two and three levels, respectively. Multiple regression analyses were performed to determine the dependency of coating thickness and porosity on the parameters selected in the first and second set of trials. Since minimum porosity was deemed more important for EBCs than thickness considerations, the parameter levels resulting in the lowest porosity were selected to run a third confirmatory set of trials.

A D-optimal design was used to optimize in-flight particle temperature and velocity, and oxide content and porosity of atmospheric plasma-sprayed In625 coatings (Ref 44). The factor effects investigated included (i) powder grain size (25 or 78 μm), (ii) stand-off distance (50 or 75 mm), (iii) powder feed rate (28 or 48 g/min), (iv) arc current (550 or 750 A), (v) argon gas flow rate (55 or 65 slpm), and (vi) hydrogen gas flow rate (0 or 2 slpm). Eight runs were sufficient to develop a model to estimate oxide content and porosity. Both in-flight particle temperature and velocity were found to be significantly determined at 95% confidence level only be the powder grain size. With the results of the first set of experiments empirical model equations for the oxide content, the porosity and the coating hardness were formulated and validated by a second set of experiments with extended levels of powder feed rate, arc current, and argon and hydrogen gas flow rates. From this, it was concluded that oxygen content was strongly (negatively) influenced at a 95% confidence level by the powder particle size, and moderately (positively) by the stand-off distance, and the argon gas flow rate. Coating porosity showed a weak negative dependence on the stand-off distance, and likewise weak positive dependence on powder grain size and arc current. Optimum spray conditions produced coatings with $<4\%$ oxide content, $<2.5\%$ porosity, and 200 HK hardness.

To determine the effects of processing parameters on three properties of small particle plasma-sprayed alumina coatings, i.e., permeability, hardness, and thickness, first a fractional factorial 2^{6-3} screening study was conducted. Based on the results, a D-optimal design with 12 runs was executed to probe the effects of four variables (plasma power, spray distance, total plasma gas flow rate, carrier gas flow rate) at three levels each. It was found that the optimum conditions for low permeability did not correlate with those for high hardness due to formation of defect structures generated as a result of copious splashing during splat formation (Ref 45).

2.6 Other Designs

The uniform design of experiment (UDE) methodology was developed starting from principles of number theory (Ref 46) by reducing the complete combination of experimental parameters to fewer experimental runs uniformly distributed within the parameter space. Compared with the conventional SDEs methods such as the Taguchi and orthogonal design methods, the UDEs method further reduces the number of experiment trials involving a large number of factors that are arranged into larger numbers of factor grades. This technique is, therefore, particularly suitable to optimize thermally sprayed coating properties involving many process parameters.

A table U_{10} ($10^2 5^3$) of UDEs was employed to optimize the properties of TiN coatings deposited by APS on AISI 304K stainless steel substrates (Ref 47). The effect of five process parameters (arc current, powder feed rate, argon gas flow rate, hydrogen gas flow rate, and spray distance) on five responses (deposition efficiency, porosity, oxygen content, microhardness, and fracture toughness) were estimated. The process parameters were graded into ten

(10^2: arc current between 460 and 550 A; powder feed rate between 20.0 and 47.8 g/min) and five (5^3: argon gas flow rate between 30 and 50 slpm; hydrogen gas flow rate between 4 and 12 slpm; spray distance between 90 and 130 mm) levels and incorporated into ten spray trials; the other process parameters were held constant. There were significant linear relationships between deposition efficiency, oxide content, microhardness, and fracture toughness. Combinations of low argon flow rate (30 slpm), high hydrogen flow rate (12 slpm), and a long spray distance (130 mm) are best suited to achieve optimum values of deposition efficiency (45%), porosity (3.6%), oxide content (24.2% relative), microhardness (775 kg/mm^2), and fracture toughness (2 MPa$\sqrt{m}$).

Applying an identical U_{10} ($10^2 5^3$) statistical design approach with the five process parameters arc current, powder feed rate, argon gas flow rate, hydrogen gas flow rate, and spray distance, the deposition efficiency, porosity, and microhardness of Y-stabilized zirconia coatings were optimized. Argon and hydrogen gas flow rates were found to be the most significant parameters (Ref 48).

2.7 Process Mapping, Modeling, Expert Systems

The examples of application of SDE methodology described above confirm amply the strong predictive power of these techniques. Even though parameter validation has to be performed and adapted to industrial requirements of TQM in conjunction with the powerful tools of process mapping (Ref 49-55), numerical simulation (Ref 56-60), high throughput screening (Ref 61), and application of expert systems (Ref 62-65), SDE provides a relatively quick, easy and economical assessment of the dependence of desired coating properties on a potentially large number of independent plasma spray parameters. In particular, it is very easy to comprehend the anatomy of the designs and to relate causes and responses by simple algorithms. However, the attainment of optimum coating properties will in many cases require more than just controlling the spray parameters since frequently contradictory settings of parameters are called for to optimize coatings for several properties simultaneously thus necessitating compromises. Hence introduction of auxiliary systems (pre-treatment, post-treatment, other control systems) is needed that control the surface state of the coatings and/or the energy level of the total system by providing additional degrees of freedom (Ref 66).

Some information is available in the literature dealing with meta-analysis of datasets from published statistical experiments. In particular, Frey et al. (Ref 67) provided guidelines for the selection of experimental design strategies. Based on meta-analysis of the results of detonation-sprayed alumina coatings (Ref 19), it could be concluded that if experimental error is small, i.e., less than a quarter of the factor effect, or the interaction among control factors are large, i.e., more than one-quarter of all factor effects, than rather surprisingly an adaptive one-at-a-time strategy tends to achieve greater gains than provided by orthogonal arrays. Investigation of regularities in the data structure of factorial designs using 113 published datasets (Ref 68) revealed the importance of *effect sparsity*, i.e., the observation that generally a small number of parameters is statistically significant, *hierarchical ordering*, i.e., the observation that main effects tend to be larger than two-factor interactions, two-factor interactions tend to be larger than three-factor interactions, etc., and *effect heredity* (*inheritance*), i.e., the observation that in order for an interaction to be significant at least one of its parent main factor should be significant. Considering these regularities in the selection of appropriate experimental designs will greatly aid experimental economy.

Parameter optimization by SDEs is a vital step in process control when moving to more elaborate approaches based on principles of artificial intelligence (AI) such as artificial neuronal network analysis (ANNA) and fuzzy logic control (FLC).

3. Artificial Neuronal Network Analysis

The responses of coating properties to variations in input parameters are complex and in most cases strongly nonlinear (see above). Accordingly, to recognize parameter interactions, correlations, and individual effect on coating properties, a robust methodology is required (Ref 69) that also enables to respond to parameter constraints based on economic and equipment considerations. Such a methodology has been found in ANNA based on database training implemented by a learning algorithm and supported by a set of experiments to predict property-parameter evolution. ANNA (Ref 70, 71) offers several advantages over the classical SDEs strategy. While treatment of nonlinear (quadratic) behavior of the response function Y in SDE requires a polynomial for p variables of the form

$$Y = b_0 + \sum_{i=1}^{p} b_i x_i + \sum_{i=1,j=1}^{p} b_{ij} x_{ij} + \sum_{j=1}^{p} b_{ii} x_i^2 \qquad \text{(Eq 5)}$$

The response polynomial required for ANN optimization of one output parameter Y depending on three input parameters x_i is

$$Y = a_0 \left((1 + \exp -(a_i \cdot x_i + a_{ij} \cdot x_{ij} + a_{jj} \cdot x_j^2) \right)^{-1}, \qquad \text{(Eq 6)}$$

where the four coefficients a will be adjusted during the training procedure. Accordingly, the number of experiments N_{SDE} required for a full factorial SDE is

$$N_{SDE} = (NL)^{NI}, \qquad \text{(Eq 7a)}$$

where NL is the number of experimental levels and NI the number of input parameters. The number of experiments required for ANNA is smaller and yields

$$N_{ANN} = a \cdot NW = a \cdot (NI + NO)^{\alpha}, \qquad \text{(Eq 7b)}$$

where NW is the number of weight parameter, NI and NO are the numbers of input and output parameters, respectively, and α is the so-called layer number (dimensionality of the system) that determines the power of prediction.

Additional strengths of ANNA consist of its ability to disclose complex correlations with small structures, lack of need for prior assumptions about input/output correlations, and the advantage of using incomplete sets of experiments, i.e., missing data can be tolerated by ANNA in contrast to SDE in which the database has to be complete, and hence missing data have to be replaced by dummy values. Constraints also consist: the database has to be representative, i.e., must show a good sampling of the input/output correlation, and the phenomena represented by the predicted relationships must have a physical relevance, hence forbidding the use of canonical variables (Ref 72). Also, the mathematical treatment is more complex and involved.

The mathematical concept of an artificial neuron was first introduced by McCulloch and Pitts (Ref 73) to emulate the signal transmission by biological neurons in the brain. Neurons receive input from one or more dendrites and sum up these input signals to produce an output signal (synapse). The sums of each node are weighted. The function relating input and output is called the transfer function, introducing nonlinearity to the system. A frequently used canonical form of the transfer function is the sigmoid (logistic or Verhulst curve), but other nonlinear functions can also be used such a piecewise linear functions or step functions, e.g., the Heaviside function (antiderivative of the Dirac delta function).

A basic function underlying ANNA is the expression

$$Y_k = \varphi\left(\sum_{j=0}^{m} w_{kj} \cdot x_j\right), \qquad \text{(Eq 8)}$$

where $\varphi = \varphi(t) = 1/(1+\exp(-t))$ is the sigmoid transfer function and m is the number of inputs with signals x_0 through x_m and weights w_0 through w_m. Figure 3 shows the simple scheme how input signals x_i ($i = 0\ldots m$) are connected to the output signal Y_k ($k =$ number of layers) by the transfer function φ. The output signal Y_k propagates to the next layer ($k+1$) through a weighted synapse.

Guessasma and Coddet (Ref 72) presented an instructive example of the power of ANNA by predicting porosity levels of alumina-13% titania coatings deposited throughout execution of 19 sets of experiments with a total of 126 samples. The input parameters varied were the plasma arc current (I, 350-750 A, reference value: 530 A), the argon primary gas flow rate (A, 40-70 slpm, reference value: 54 slpm), the hydrogen secondary gas flow rate (H, 0-50 slpm, reference value: 35 slpm), the carrier gas flow rate (CG, 2.2-4.2 slpm, reference value: 3.2 slpm), and the powder feed rate (D_m, 7-22 g/min, reference value: 22 g/min). Spray distance (125 mm), spray angle (90°), injector diameter (1.8 mm), and injection distance (6 mm) were kept constant throughout.

Background information on ANNA, training and testing procedures, and implementation and adaptation to databases were discussed by Guessasma and Coddet (Ref 72; see also Ref 74). In particular, the training rule applied was provided by a quick learning algorithm considering weight update as a function of the previous and current cycles until an optimum residual error occurs (Ref 75).

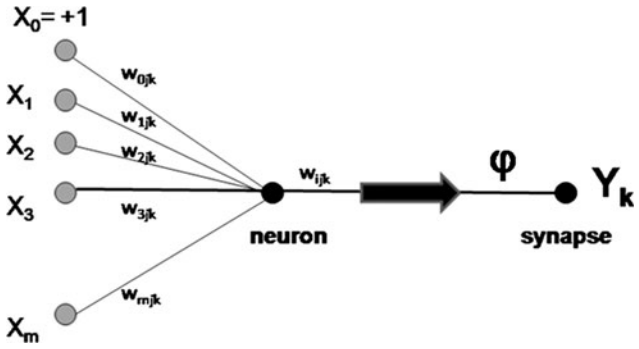

Fig. 3 Input signals X_i with weights w_{ijk} are connected to the output signal Y_k through the transfer function φ. This scheme is the graphical representation of Eq 8

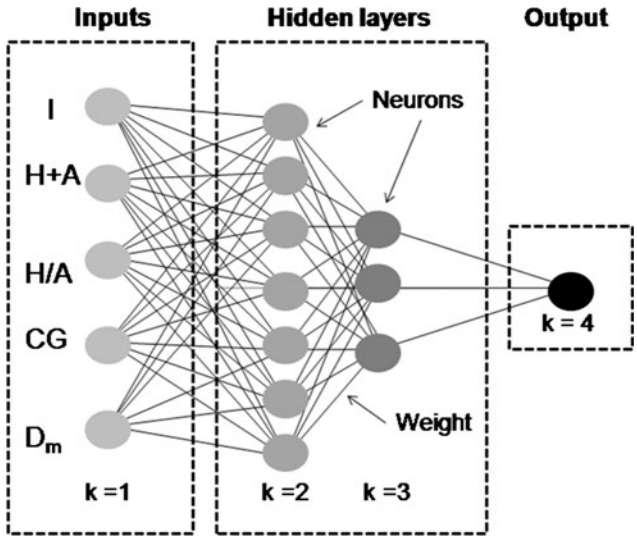

Fig. 4 Artificial neuronal network structure used to predict the porosity (output) of plasma-sprayed alumina-13% titania coatings as a function of the input parameters I, $H+A$, H/A, CG, and D_m (modified after Ref 72)

With the database obtained from the experiments described above, an optimized artificial neural network structure was developed as shown in Fig. 4. The database was divided into three parts: 50% of the experiments were assigned to fine-tune the weight parameters NW in the training stage, 27% for the test of the network configuration during the test stage, and the remainder to test the generalization of the optimized network to predict porosity values in the input parameter range outside the experimentally applied values during the prediction stage. Hence calculations were performed in the following prediction ranges: arc current $I \rightarrow$ 300-800 A; total gas flow rate $H+A \rightarrow$ 20-80 slpm; ratio of hydrogen/argon gas flow rates $H/A \rightarrow$ 0-50 slpm; carrier gas flow rate CG $\rightarrow$ 1.5-5 slpm; powder feed rate $D_m \rightarrow$ 5-60 g/min.

As shown in Fig. 4, the first layer of the ANNA ($k=1$) contains the five input parameters I, A, H, CG, and D_m, the first hidden layer ($k=2$) contains seven neurons, the

second hidden layer ($k=3$) contains three neurons, and the output layer ($k=4$) yields the predicted porosity. To compare predicted and experimental porosity values, each input parameter was varied individually, keeping the others at their reference values. Previously obtained information on the possible anatomy of the system confirmed that with only two hidden layers, a correct optimization could be obtained (Ref 76).

Using ANNA, the experimentally obtained porosity levels P (2-10%) were found to be dependent on all five input parameters to yield the following equations:

1. Arc current:

$$P(\%) = 6.26 + 3.28 \times 10^{-5} I^2 - 5.14 \times 10^{-8} I^3; \quad r^2 = 0.83$$

2. Total gas flow rate:

$$P(\%) = 7.3 + 0.01 \times (H + A); \quad r^2 = 0.42$$

3. Hydrogen/argon ratio:

$$P(\%) = 10.13 - 0.09 \times (H/A); \quad r^2 = 0.93$$

4. Carrier gas flow rate:

$$P(\%) = 16.58 - 6.34\mathrm{CG} + 1.10\mathrm{CG}^2; \quad r^2 = 0.38$$

5. Powder feed rate:

$$P(\%) = 5.45 + 0.1 D_{\mathrm{m}}; \quad r^2 = 0.93.$$

The low regression coefficients of relationships two and four were attributed to the scatter of the experimental results around the mean values.

The predicted parameter effects are 68% for input parameter I between 350 and 750 A (i.e., the predicted decrease of porosity from 9% to about 2.5% corresponds to 68%), 4% for H + A between 40 and 70 slpm, 34% for H/A between 13% and 50%, 9% for CG between 2.2 and 4.2 slpm, and 19% for D_{m} between 7 and 22 g/min. Hence the porosity of plasma-sprayed alumina-13% titania coatings decreases strongly with increasing arc current (nonlinearly) and hydrogen/argon ratio (linearly), i.e., plasma enthalpy, and decreases somewhat with decreasing powder feed rate (linearly), i.e., less cooling of the plasma jet under decreasing dense loading condition. The contributions of the total plasma gas flow rate (linearly) and the carrier gas flow rate (parabolically) are weak. Based on these results, the predicted individual control factors were arc current I, hydrogen fraction H/A, and powder feed rate D_{m}. Taking into account interaction of all parameters, the control factors were the arc current and the hydrogen fraction. Then porosity levels $<2\%$ could be achieved with the following parameter setting: $I > 425$ A, $H/A > 37.4\%$. As expected, minimum porosities are being generated by increased heat transfer in-flight from the plasma to the particles, and reduction of viscosity of the molten droplets and hence increase of the flattening ratio ξ during impact.

Artificial neural network analysis has been successfully applied to control important properties such as porosity, hardness, and wear behavior of several types of coatings including alumina-13% titania (gray alumina) (Ref 64, 72, 77-80), zirconia (Ref 81), and SiC-filled PEEK for application in novel bearings (Ref 82). Neural networks were applied to implement process control via an optical diagnostic system with the goal to increase process robustness. Parameter optimization was done by SDE considering the effects of the noise factors electrode wear and injector wear (Ref 83). Predictive control of thermal spray processing was attempted through neural networks using SDE as a training tool (Ref 84-86). In this context, it also appears worthwhile to mention a new associative classification algorithm developed for manufacturing data mining, in particular applied to control thermal spray processes. The algorithm uses elementary set concepts, information entropy, and database manipulation techniques to develop important relationships, i.e., knowledge attributes between input parameters and output responses (Ref 65).

4. Fuzzy Logic Control

This approach is rarely used to optimize the properties of plasma-sprayed coatings. Noticeable exemptions can be found in Ref 87-90. FLC is a knowledge-based methodology that translates human linguistics into an optimized model of controllable reality using a set of fuzzy rules and membership functions. It is an organized and mathematical method of handling inherently imprecise concepts such as the nonlinear dependence of the thickness of plasma-sprayed coatings on a multitude of input parameters. This uncertainty originates from the chaotic nature of the coating process in which infinitesimally small changes in the input parameters cause large and in general nondeterministic changes in the output parameter, i.e., coating properties. Nonlinearity is introduced by stochastic arc root fluctuation as well as entrainment of parcels of cold air by chaotic pulsation caused by the turbulent action of the plasma jet. As far as heat transfer is concerned, nonequilibrium distributions of the phases of plasma waves cause electromagnetic and magneto-hydrodynamic turbulences that affect the local magnetic field strength, B and the electrical current density, j. Consequently their cross-product, the Lorentz force ($j \times B$) fluctuates rapidly and with it the plasma compression (''z-pinch''). Finally, the local thermal equilibrium breaks down on a scale that is small compared to the overall volume of the plasma jet. Then, the system enters the realm of a ''*heat transfer catastrophy.*'' This phenomenon can be tentatively described in terms of stability theory by an elementary cusp catastrophy of co-dimension two (Riemann-Hugoniot catastrophy) (Ref 2).

The FLC system consists of several units including a ''fuzzificator,'' an inference engine containing a database and a rule base, and a ''defuzzificator'' (Ref 91-93). Figure 5 shows a flow chart of a fuzzy logic controller coupled with Taguchi-structured control factors designed to optimize the thickness of plasma-sprayed ZrO_2-8%Y_2O_3 TBCs (Ref 87). Coatings were deposited under

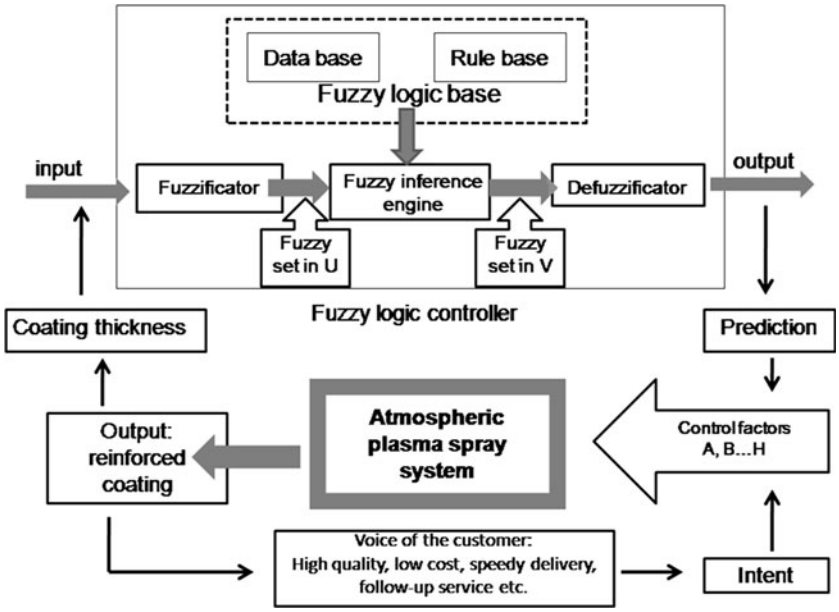

Fig. 5 Flow chart of a fuzzy logic controller coupled with Taguchi-structured control factors (after Ref 87)

statistical variation of seven input parameters at three levels and one parameter at two levels according to an orthogonal $L_{18}(2^1 3^7)$ fractional Taguchi design. The operating parameters X_i were the number of traverses (A: 5; 8), the accelerating voltage (B: 65; 70; 75 V), the arc current (C: 550; 600; 650 A), the traverse speed of the plasmatron (D: 20; 25; 30 mm/s), the stand-off distance (E: 80; 100; 120 mm), the powder feed rate (F: 20; 25; 30 g/min), the carrier gas flow rate (G: 5; 6; 7 slpm), and the primary plasma gas flow rate (H: 50; 55; 60 slpm).

According to Jean et al. (Ref 87), a fuzzy system is defined as

$$f : U = \bigcup_{i=1}^{n} U_i \subset R^n \Rightarrow V \subset R, \qquad \text{(Eq 9)}$$

where U and V are input and outputs, respectively, and R refers to the rule base. Each fuzzy rule R can be expressed by a Boolean conditional 'If-Then' statement as follows:

$$\text{Rule i : If input parameter } X_1 \text{ is } A_{i1} \text{ and } X_2 \text{ is } A_{i2} \text{ and } \ldots X_n \text{ is } A_{in} \text{ then } Y_i \text{ is } B_i, \qquad \text{(Eq 10)}$$

for $i = 1, 2, \ldots m$. The terms A_{in} are linguistic sets* associated with the inputs X_n, the output Y_i is determined by the linguistic terms B_i. The range of inputs were partitioned into the three linguistic sets ***S*** (small), ***M*** (medium), and ***L*** (large), the range of outputs into a set of nine membership functions: ***SS*** (small small), ***VS*** (very small), ***S*** (small), ***SM*** (small medium), ***M*** (medium), ***ML*** (medium large), ***L*** (large), ***VL*** (very large), and ***LL*** (large large). The Mamdani centroid inference method (Ref 94) was applied to defuzzify the output membership functions to obtain a valid prediction (see Fig 5).

From ANOVA, the three factors accelerating voltage (B), stand-off distance (E), and carrier gas flow rate (G) were found to affect the coating thickness most, accounting for 78.6% of the total experimental variance whereby the individual percent contributions were about equal at 26%. Hence these highly significant factors were assigned to a fuzzy logic controller with 27 fuzzy rules to predict the outputs. From historical data, it was concluded that a coating thickness of 50 μm was most desirable to guarantee maximum coating adhesion to the substrate.** Applying the logic rules along with the Mamdani centroid inference (Ref 94), the linguistic and membership values for the outputs can be determined. In the particular case described in Ref 87 out of the 27 fuzzy rules, only four membership functions "fired," i.e., fulfilled the requirements to accommodate the three significant factors to minimize the coating thickness to a value as close as possible to the desired 50 μm as indicated by a linguistic output value SS. These rules are as follows:

Rule 6: If (B is ***S***, E is ***M***, G is ***L***) then coating thickness ***SS***.

Rule 9: If (B is ***S***, E is ***L***, G is ***L***) then coating thickness is ***SS***.

Rule 15: If (B is ***M***, E is ***M***, G is ***L***) then coating thickness is ***SM***.

Rule 18: If (B is ***S***, E is ***L***, G is ***L***) then coating thickness is ***SS***.

*These linguistic terms are at least semantically akin to 'discrete' variables in the much less involved screening designs of Plackett-Burman type.

**It should be mentioned that adhesion of plasma-sprayed coatings is not just a function of coating thickness which controls the residual stress level, but other factors such as splat cohesion, substrate roughness, temperature of the substrate, properties of the bond coats, level of impurities and degree of oxidation play likewise important roles.

The coating thickness for the input parameter set with A → ***L***, B → ***M***, C → ***M***, D → ***L***, E → ***L***, F → ***S***, G → ***L***, H → ***S*** has been measured to be 51.67 μm, very close to the design value of 50 μm which compares favorably to the defuzzyfied values of 51.41 μm. The fact that for this parameter combination the signal-to-noise ratio shows with −12.3 db, the largest value of all tests confirms that the FLC design accurately predicted the target coating thickness.

5. Conclusion

TQM of thermally sprayed coatings involves a chain of events that must be implemented to arrive at a high-quality process that will result in a high-quality product that consistently meets demand and expectations of the customers. The quality tools of this chain link research, development, and product: *Statistical Design of Experiments* (SDE/SES) identifies those plasma spray parameters that significantly influence coating performance, process-based *Statistical Process Control* including principles of AI such as neuronal networks and fuzzy logic ensures consistency in the industrial production of coatings through Taguchi-type control designs, and the *Quality Function Deployment* translates consumer demands into technical reality, i.e., engineering factors.

Acknowledgments

The author of this review paper is indebted to several colleagues including Christian Coddet (Belfort, France), Thomas Coyle (Toronto, Canada), Rogerio Lima (Boucherville, Canada), Sanjay Sampath (Stony Brook, USA), and P. Saravanan (Coimbatore, India) for providing access to their published work. Thanks are also due to Hans D. Lehmann (Görlitz, Germany) for bibliographical assistance.

References

1. S. Bisgaard, Optimizing Thermal Spray Processes—Going Beyond Taguchi Methods, *Proc. 3rd NTSC*, Long Beach, CA, May 20-25, 1990, p 661-668
2. R.B. Heimann, *Plasma Spray Coating: Principles and Applications*, 2nd ed., Wiley-VCH, Weinheim, 2008
3. C. Pierlot, L. Pawlowski, M. Bigan, and P. Chagnon, Design of Experiments in Thermal Spraying, *Surf. Coat. Technol.*, 2008, **202**, p 4483-4490
4. G. Pouskouleli and T.A. Wheat, Total Quality Management (TQM): Recipe for Survival, *Transactions 17th CUICAC Workshop 'Ceramic Coatings—A Solution Towards Reducing Wear and Corrosion*, R.B. Heimann, Ed., 2 Oct, Laval University, 1991
5. R.L. Plackett and J.P. Burman, The Design of Optimum Multifactorial Experiments, *Biometrika*, 1946, **33**(4), p 305-325
6. A. Arcondéguy, G. Gasgnier, G. Montavon, B. Pateyron, A. Denoirjean, A. Grimaud, and C. Huguet, Effects of Spraying Parameters onto Flame-Sprayed Glaze Coating Structures, *Surf. Coat. Technol.*, 2008, **202**(18), p 4444-4448
7. F. Yates, "The Design and Analysis of Factorial Experiments," Techn. Comm. 35, Imperial Bureau Soil Sci., Harpenden, UK, 1937
8. J.S. Hunter, The Inverse Yates Algorithm, *Technometrics*, 1966, **8**, p 177-183
9. U.V. Diccar, "Plasma Spray Coatings for Polymer Composites," Master Thesis, Wichita State University, December 2006
10. E. Perez,"Development of APS MCrAlY Dense Bond Coats," Report, University of Central Florida, 2006. www.clemson.edu/scies/UTSR/FellowPerezSUM6-2006.pdf
11. G.E.P. Box and J.S. Hunter, The 2^{k-p} Fractional Factorial Designs, *Technometrics*, 1961 **3**(3), p 311-331, 449-458
12. M. Erne,"Optimierung der Dichte, Dicke und Oberflächenrauheit APS-gespritzter Chrom- oxid-Korrosionsschutzschichten," Unpublished 4th Year Thesis, Technische Universität Bergakademie Freiberg, 2004 (http://www.wissen24.de/vorschau/25257.html)
13. B.D. Sartwell, K.O. Legg, J. Schell, J. Sauer, P. Natishan, D. Dull, J. Falkowski, P. Bretz, J. Devereaux, C. Edwards, and D. Parker, "Validation of HVOF WC/Co Thermal Spray Coatings as a Replacement for Hard Chrome Plating on Aircraft Landing Gear," Naval Research Lab., Report No. NRL/MR/6170-04-8762, 2004, 280 pp
14. G. Taguchi and S. Konishi, *Taguchi Methods: Orthogonal Arrays and Linear Graphs*, ASI Press, Dearborn, MI, 1987
15. D.C. Montgomery, *Design and Analysis of Experiments*, Wiley, New York, 1991
16. P. Saravanan, V. Selvarajan, M.P. Srivastava, S.V. Joshi, and G. Sundararajan, Influence of Spraying Variables on Structure and Properties of Plasma Sprayed Alumina Coatings, *Brit. Ceram. Trans*, 2000, **99**(6), p 241-247
17. P. Saravanan, V. Selvarajan, D. Srinivasa Rao, S.V. Joshi, and G. Sundararajan, Application of Taguchi Method to the Optimization of Detonation Spraying Process, *Mater. Manufact. Process.*, 2000, **15**(1), p 139-153
18. P. Saravanan, V. Selvarajan, M.P. Srivastava, D.S. Rao, S.V. Joshi, and G. Sundararajan, Study of Plasma- and Detonation Gun-Sprayed Alumina Coatings Using Taguchi Experimental Design, *J. Thermal Spray Technol.*, 2000, **9**(4), p 505-512
19. P. Saravanan, V. Selvarajan, S.V. Joshi, and G. Sundararajan, Experimental Design and Performance Analysis of Alumina Coatings Deposited by a Detonation Spray Process, *J. Phys. D Appl. Phys.*, 2001, **34**, p 131-140
20. A. Kucuk, C.C. Berndt, U. Senturk, and R.S. Lima, Characterization of Mechanical Properties of TBCs via a Taguchi Experimental Design, *Proc. 1st ITSC, Thermal Spray Surface Engineering via Applied Research*, Montreal, QC, Canada, May 9-11, 2000, p 1211-1217
21. M. Gell, L. Xie, X. Ma, E.H. Jordan, and N.P. Padhure, Highly Durable Thermal Barrier Coatings Made by the Solution Precursor Plasma Spray Process, *Surf. Coat. Technol.*, 2004, **177-178**, p 97-102
22. J. Cizek, K.A. Khor, and Z. Prochazka, Influence of Spraying Conditions on Thermal and Velocity Properties of Plasma Sprayed Hydroxyapatite, *Mater. Sci. Eng. C*, 2007, **27**(2), p 340-344
23. H.K. Kim, J.W. Jang, and C.H. Lee, Surface Modification of Implant Materials and its Effect on Attachment and Proliferation of Bone Cells, *J. Mater. Sci. Mater. Med.*, 2004, **15**(7), p 825-830
24. G. Gibbons and R. Hansell, Down-Selection and Optimization of Thermal-Sprayed Coatings for Aluminum Mould Tool Protection and Upgrade, *J. Thermal Spray Technol.*, 2006, **15**(3), p 340-347
25. F. Tarasi, M. Medraj, A. Dolatabadi, J. Oberste-Berghaus, and C. Moreau, Effective Parameters in Axial Injection Suspension Plasma Spray Process of Alumina-Zirconia Ceramics, *J. Thermal Spray Technol.*, 2008, **17**(5-6), p 685-691
26. R.B. Heimann, D. Lamy, and T. Sopkow, Optimization of Vacuum Plasma Arc Spray Parameters of 88WC12Co Alloy Coatings Using a Statistical Multifactorial Design Matrix, *J. Can. Ceram. Soc.*, 1990, **59**(3), p 49
27. J. Grum and Z. Bergant, The Optimisation of Powder Flame-Spraying Parameters Using a Taguchi Method, *Int. J. Microstruct. Mater. Prop.*, 2008, **3**(4-5), p 682-700
28. G. Bertrand, P. Bertrand, P. Roy, C. Rio, and R. Mevrel, Low Conductivity Plasma Sprayed Thermal Barrier Coating Using Hollow PSZ Spheres: Correlation Between Thermophysical

Properties and Microstructure, *Surf. Coat. Technol.*, 2008, **202**(10), p 1994-2001
29. G.E.P. Box and D.W. Behnken, Some New Three Level Designs for the Study of Quantitative Variables, *Technometrics*, 1960, **2**, p 455-475
30. F. Cipri, C. Bartuli, T. Valente, and F. Casadei, Electromagnetic and Mechanical Properties of Silica-Aluminosilicates Plasma Sprayed Composite Coatings, *J. Thermal Spray Technol.*, 2007, **16**(5-6), p 831-838
31. B.T. Lin, M.D. Jean, and J.H. Chou, Using Response Surface Methodology for Optimizing Deposited Partially Stabilized Zirconia in Plasma Spraying, *Appl. Surf. Sci.*, 2007, **253**(6), p 3254-3262
32. A. Schuppert and A. Ohrenberg, ''Method and Computer for Experimental Design,'' EP1499930, 2005
33. G.E.P. Box and K.B. Wilson, On the Experimental Attainment of Optimum Conditions, *J. Roy. Statist. Soc.*, 1951, **13**, p 1-45
34. J. Bohm, M. Bohm, and R.B. Heimann, Voronoi Polyhedra: A Useful Tool to Determine the Symmetry and Bravais Class of Crystal Lattices, *Cryst. Res. Technol.*, 1996, **31**(8), p 1069-1075
35. J. Zimmermann, ''Untersuchungen zur Haftfestigkeit und Rauheit plasmagespritzter Cr_2O_3-Schichten,'' Unpublished 4th Year Thesis, Technische Universität Bergakademie Freiberg, 2000
36. G. Reisel and R.B. Heimann, Correlation Between Roughness of Plasma-Sprayed Chromium Oxide Coatings and Powder Grain Size Distribution: A Fractal Approach, *Surf. Coat. Technol.*, 2004, **183**, p 215-221
37. Y. Wang and T.W. Coyle, Optimization of Solution Precursor Plasma Spray Process by Statistical Design of Experiment, *J. Thermal Spray Technol.*, 2008, **17**(5-6), p 692-699
38. H.O. Hartley, Smallest Composite Designs for Quadratic Response Surfaces, *Biometrics*, 1959, **15**(4), p 611-624
39. A. Yudee, A. Sopadang, S. Wirojanupatump, and S. Jiansirisomboon, Aluminium-12wt% Silicon Coating Prepared by Thermal Spraying Technique: Part 1. Optimization of Spray Condition Based on a Design of Experiments, *Songklanakarin J. Sci. Technol.*, 2006, **28**(2), p 431-439
40. B.T. Neyer, A D-Optimality-Based Sensitivity Test, *Technometrics*, 1994, **36**(1), p 61-70
41. C. Pumplün, S. Rüping, K. Morik, and C. Weihs, ''D-Optimal Plans in Observational Studies,'' Report SFB 475 (Reduction of Complexity in Multivariate Data Structures), University Dortmund, Germany, 2005
42. M. Moldovan, C.M. Weyant, D.L. Johnson, and K.T. Faber, Tantalum Oxide Coatings as Candidate Environmental Barriers, *J. Thermal. Spray Technol.*, 2004, **13**(1), p 51-56
43. H.S. Haller, *Experimental Design Optimizer (Software Manual)*, Harold S. Haller & Co, Cleveland, OH, 1999
44. F. Azarmi, T.W. Coyle, and J. Mostaghimi, Optimization of Atmospheric Plasma Spray Process Parameters Using a Design of Experiment for Alloy 625 Coatings, *J. Thermal. Spray Technol.*, 2008, **17**(1), p 144-155
45. J.F. Li, H. Liao, B. Normand, C. Codier, G. Maurin, J. Foct, and C. Coddet, Uniform Design Method for Optimization of Process Parameters of Plasma-Sprayed TiN Coatings, *Surf. Coat. Technol.*, 2003, **176**(1), p 1-13
46. K.T. Fang and Y. Wang, *Number-Theoretic Methods in Statistics*, Chapman and Hall, London, 1994
47. J.F. Li, H.L. Liao, C.X. Ding, and C. Coddet, Optimizing the Plasma Spray Process Parameters of Yttria Stabilized Zirconia Coatings Using a Uniform Design of Experiments, *J. Mater. Proc. Technol.*, 2005, **160**(1), p 34-42
48. J.R. Mawdsley, Y.J. Su, K.T. Faber, and T.F. Bernecki, Optimization of Small-Particle Plasma-Sprayed Alumina Coatings Using Designed Experiments, *Mater. Sci. Eng. A*, 2001, **308**, p 189-199
49. S. Sampath, X. Jiang, A. Kulkarni, J. Matejicek, D.L. Gilmore, and R.A. Neiser, Development of Process Maps for Plasma Spray: Case Study for Molybdenum, *Mater. Sci. Eng. A*, 2003, **348**, p 54-66
50. A. Vaidya, T. Streibl, L. Li, S. Sampath, O. Kovarik, and R. Greenlaw, An Integrated Study of Thermal Spray Process-Structure-Property Correlations: A Case Study for Plasma Sprayed Molybdenum Coatings, *Mater. Sci. Eng. A*, 2005, **403**(1-2), p 191-204
51. X. Jiang, J. Matejicek, A. Kulkarni, H. Herman, S. Sampath, D. Gilmore, and R. Neiser, ''Process Maps for Plasma Spray Part II: Deposition and Properties,'' Report SAND2000-0802c, 2000, p 1-7
52. E. Turunen, T. Varis, T.E. Gustavson, J. Keskinen, T. Fält, and S.P. Hannula, Parameter Optimization of HVOF Sprayed Nanostructured Alumina and Alumina-Nickel Composite Coatings, *Surf. Coat. Technol.*, 2006, **200**(16-17), p 4987-4994
53. W. Zhang and S. Sampath, A Universal Method for Representation of In-Flight Particle Characteristics in Thermal Spray Processes, *J. Thermal Spray Technol.*, 2009, **18**(1), p 23-24
54. A. Vaidya, V. Srinivasan, T. Streibl, M. Friis, W. Chi, and S. Sampath, Process Maps for Plasma Spraying of Yttria-Stabilized Zirconia: An Integrated Approach to Design, Optimization and Reliability, *Mater. Sci. Eng. A*, 2008, **497**(1-2), p 239-253
55. J.C. Fang, H.P. Zeng, W.J. Wu, Z.Y. Zhao, and L. Wang, Prediction of In-Flight Particle Behaviors in Plasma Spraying, *J. Achiev. Mater. Manufact. Eng.*, 2006, **18**(1-2), p 283-286
56. H.B. Xiong, L.L. Zheng, and T. Streibl, A Critical Assessment of Particle Temperature Distribution During Plasma Spraying: Numerical Studies for YSZ, *Plasma Chem., Plasma Proc.*, 2006, **26**(1), p 53-72
57. B. Liu, T. Zhang, and D.T. Gawne, Computational Analysis of the Influence of Process Parameters on the Flow Field of a Plasma Jet, *Surf. Coat. Technol.*, 2000, **132**(2-3), p 202-216
58. I. Ahmed and T.L. Bergman, Optimization of Plasma Spray Processing Parameters for Deposition on Nanostructured Powders for Coating Formation, *J. Fluid Eng.*, 2006, **128**(2), p 394-401
59. C. Le Bot and E. Arquis, Numerical Study of the Solidification of Successive Thick Metal Layers, *Int. J. Thermal Sci.*, 2009, **48**(2), p 412-420
60. S. Hossainpour and A.R. Binesh, A CFD Study of Sensitive Parameter Effects on the Combustion in a High Velocity Oxygen Fuel Thermal Spray Gun, *Proc. World Acad. Sci. Eng. Technol.*, 2008, **31**, p 213-220
61. R. Cesaretti, High Throughput Screening of Coatings, Adhesive, Sealants and Elastomer (CASE) Formulations, *Symyx Global Symp.*, Philadelphia, May 12-14, 2009, p 1
62. P. Seyffarth, A. Scharff, F.W. Bach, L.A. Josefiak, B. Bouaifi, and T. Schlennstedt, SprayWare-Beratungssystem für den Oberflächenschutz durch thermisches Spritzen, *Schweissen und Schneiden*, 2002, **54**, p 192-199
63. F.I. Trifa, G. Montavon, and C. Coddet, Model-Based Expert System for Design and Simulation of APS Coatings, *J. Thermal Spray Technol.*, 2007, **16**(1), p 128-139
64. S. Guessasma, G. Montavon, P. Gougeon, and C. Coddet, Designing Expert Systems Using Neural Computation in View of the Control of Plasma Spray Processes, *Mater. Design*, 2003, **24**(7), p 497-502
65. Y. Siradeghyan, A. Zakarian, and P. Mohanty, Entropy-Based Associative Classification Algorithm for Mining Manufacturing Data, *Int. J. Comput. Integr. Manufact.*, 2008, **21**(7), p 825-838
66. C. Coddet, On the Use of Auxiliary Systems During Thermal Spraying, *Surf. Coat. Technol.*, 2006, **201**(5), p 1969-1974
67. D.D. Frey, F. Engelhardt, and E.M. Greitzer, A Role for ''One-Factor-at-a-Time'' Experimentation in Parameter Design, *Res. Eng. Design*, 2003, **14**, p 65-74
68. X. Li, N. Sudarsanam, and D.D. Frey, Regularities in Data from Factorial Experiments, *Complexity*, 2006, **11**(5), p 32-45
69. S. Guessasma, G. Montavon, and C. Coddet, Modeling of the APS Plasma Spray Process Using Artificial Neural Networks: Basis, Requirements and an Example, *Comput. Mater. Sci.*, 2004, **29**(3), p 315-333
70. M.M. Nelson and W.T. Illingworth, *A Practical Guide to Neural Nets*, 3rd ed., Addison-Wesley, Reading, MA, 1991
71. J.B. Tenenbaum and W.T. Freeman, Separating Style and Content, *Proc. Advanc. Neural Process Information Systems*, M.C. Mozer, M.I. Jordan, and T. Petsche, Ed., Vol. 9, Part IV, The MIT Press, Cambridge, MA, USA, 1997, p 662–668
72. S. Guessasma and C. Coddet, Neural Computation Applied to APS Spray Process: Porosity Analysis, *Surf. Coat. Technol.*, 2005, **197**, p 85-92

73. W. McCulloch and W. Pitts, A Logical Calculus of Ideas Immanent in Nervous Activity, *Bull. Math. Biophys.*, 1943, **7**, p 115-133
74. L. Wang, J.C. Fang, Z.Y. Zhao, and H.P. Zeng, Application of Backward Propagation Network for Forecasting Hardness and Porosity of Coatings by Plasma Spraying, *Surf. Coat. Technol.*, 2007, **201**(9-11), p 5085-5089
75. D. Patterson, *Artificial Neural Networks*, Prentice Hall, Singapore, 1996
76. S. Guessasma, G. Montavon, P. Gougeon, and C. Coddet, On the Neural Network Concept to Describe the Thermal Spray Deposition Process: Correlation Between In-Flight Particles Characteristics and Processing Parameters, *Proc. ITSC 2002*, E. Lugscheider and P.A. Kammer, Ed., DVS-Verlag, Düsseldorf, Germany, 2002, p 453-458
77. S. Guessasma, G. Montavon, and C. Coddet, Plasma Spray Process Modeling Using Artificial Neural Networks: Application to Al_2O_3-TiO_2 (13% by Weight) Ceramic Coating Structure, *J. Phys. IV France*, 2004, **120**, p 363-370
78. S. Guessasma, Z. Salhi, G. Montavon, P. Gougeon, and C. Coddet, Artificial Intelligence Implementation in the APS Process Diagnostics, *Mater. Sci. Eng. B*, 2004, **110**(3), p 285-295
79. S. Guessasma, M. Bounazet, and P. Nardin, Neural Computation Analysis of Alumina-Titania Wear Resistance Coating, *Int. J. Refract. Met. Hard Mater.*, 2006, **24**(3), p 240-246
80. A.F. Kanta, G. Montavon, M.P. Planche, and C. Coddet, Artificial Intelligence Computation to Establish Relationships Between APS Process Parameters and Alumina-Titania Coating Properties, *Plasma Chem. Plasma Proc.*, 2008, **28**, p 249-262
81. M.D. Jean, B.T. Lin, and J.H. Chou, Application of an Artificial Neural Network for Simulating Robust Plasma-Sprayed Zirconia Coatings, *J. Am. Ceram. Soc.*, 2008, **91**(5), p 1539-1547
82. G. Zhang, S. Guessasma, H. Liao, C. Coddet, and J.M. Bordes, Investigation of Friction and Wear Behaviour of SiC-Filled PEEK Coating Using Artificial Neural Networks, *Surf. Coat. Technol.*, 2006, **200**(8), p 2610-2617
83. K. Bobzin, F. Ernst, J. Zwick, K. Richardt, R. Schmitt, and J. Dören, Increase of Process Robustness Through Offline Process Control and Noise Factor Influence Reduction, *Proc. 2007 Intern. Thermal Spray Conf. (ISTC)*, Beijing, China, May 14-16, 2007, p 855-859
84. J. Dören, ''Quality Management and Neural Networks: An Approach for Predictional Control of Thermal Spray Processes,'' Ph.D. Dissertation, Faculty of Mechanical Engineering, RWTH Aachen, Germany, 2007. URL: http://darwin.bth.rwth-aachen.de/opus3/volltexte/2007/1986
85. S. Guessasma, G. Montavon, and C. Coddet, Neural Networks, Design of Experiments and Other Optimization Methodologies to Quantify Parameter Dependence of Atmospheric Plasma Spraying, *Thermal Spray 2003: Advancing The Science & Applying the Technology*, C. Moreau and B. Marple, Ed., Orlando, FL, May 5-8, 2003, p 939-948
86. A.F. Kanta, G. Montavon, M. Vardelle, M.P. Planche, C.C. Berndt, and C. Coddet, Artificial Neural Networks vs. Fuzzy Logic: Simple Tools to Predict and Control Complex Processes-Application to Plasma Spray Processes, *J. Thermal Spray Technol.*, 2008, **17**(3), p 365-376
87. M.D. Jean, B.T. Lin, and J.H. Chou, Design of a Fuzzy Logic Approach for Optimization Reinforced Zirconia Depositions Using Plasma Sprayings, *Surf. Coat. Technol.*, 2006, **201**(6), p 3129-3138
88. A.F. Kanta, G. Montavon, M.P. Planche, and C. Coddet, Prospect for Plasma Spray Processes On-Line Control Via Artificial Intelligence (Neural Networks and Fuzzy Logic), *Thermal Spray 2006: Science, Innovation, and Application, Proc. 2006 ITSC*, Seattle, WA, May 15-18, 2006, p 1027-1033
89. A.F. Kanta, G. Montavon, M.P. Planche, and C. Coddet, Fuzzy Logic Analysis of Alumina-Titania Deposition Yield During APS Process, *J. Thermal Spray Technol.*, 2007, **16**, p 913-918
90. A.F. Kanta, G. Montavon, M.P. Planche, and C. Coddet, In-Flight Particle Characteristics Control by Implementing a Fuzzy Logic Controller, *Surf. Coat. Technol.*, 2008, **202**, p 4479-4482
91. L.A. Zadeh, Fuzzy Sets, *Inform. Control*, 1965, **8**(3), p 338-353
92. H.J. Zimmermann, *Fuzzy Set Theory*, 2nd ed., Kluwer, Boston, 1991
93. T.J. Ross, *Fuzzy Logic with Engineering Applications*, Wiley, Chichester, 2004
94. E.H. Mamdani and S. Assilian, An Experiment in Linguistic Synthesis with a Fuzzy Logic Controller, *IEEE Trans. Comput.*, 1975, **26**(12), p 1182-1191